Adaptive and Unconventional Strategies for Engine Knock Control

Donald Selmanaj, Giulio Panzani, Stijn van Dooren, Jonatan Rosgren and Christopher Onder

Abstract

Knock is an undesirable phenomenon affecting gasoline spark-ignition (SI) engines. In order to maximize engine efficiency and output torque while limiting the knock rate, the spark timing should be adequately controlled. This paper focuses on closed-loop knock control strategies. The proposed control strategies, compared to conventional approaches, show an improved performance while remaining simple to use, implement, and tune. First, a deterministic controller which employs a logarithmic increase of the spark timing proves to outperform the conventional strategy in terms of spark timing average and variance. Second, a stochastic adaptive strategy that is meant to assist the deterministic controller is introduced. Due to this extension, the average and the variance of the spark timing are improved while preserving the easy tuning and the fast reaction times of the deterministic strategy. Throughout the paper, all the knock controllers are compared with a conventional deterministic strategy and with a recently proposed stochastic one. The advantages of the proposed approaches are confirmed both by simulation and by experimental data collected at a test bench.

Index Terms

knock control, SI engines, adaptive, stochastic.

This project has received funding from the European Union's Horizon 2020 research and innovation programme under grant agreement No: 634135-HERCULES-2.

Donald Selmanaj, Stijn van Dooren and Christopher Onder are with the Institute for Dynamic Systems and Control, ETH Zurich, Sonneggstrasse 3, CH-8092 Zurich, Switzerland.

Giulio Panzani is with the Dipartimento di Elettronica, Informazione e Bioingegneria, Politecnico di Milano, Piazza L. da Vinci, 32, 20133, Milano, Italy.

Jonatan Rosgren is with Wärtsilä Finland Oy, FIN-65101, Vaasa, Finland

I. Introduction

The phenomenon of knock is a major limitation for SI engines. Knock has its name from the audible noise that results from autoignitions in the unburned part of the gas. It causes undesired pressure oscillations in the combustion chamber. In order to avoid knock, the engine has to be run in a sub-optimal way with respect to efficiency. In addition to limiting the compression ratio and lowering the levels of pressure and temperature, preventing knock requires the spark timing to be delayed [1]. Closed-loop knock control systems acting on spark timing are thus crucial in order to maximize the engine efficiency while limiting the knock rate.

Knock sensing is a key component for knock control systems. On the one hand, considerable research efforts have been dedicated to the problem of knock detection [2]–[5] by processing different types of measurements to produce knock metrics [6]–[15]. On the other hand, knock control strategies have received less attention. The most trivial strategy consists of rapidly retarding the spark timing if a knock event is observed, and slowly advancing the timing during non-knocking cycles [16]. This strategy is referred to in literature as the conventional knock control strategy and is widely used in industrial applications. The conventional strategy is easy to implement and tune, but it results in late average and a high variance of the spark timing.

More advanced methods are based on the concept of margin (or distance) from the knocking condition. Instead of acting on knock events, these approaches relate the knock intensity to measurement data obtained during non-knocking cycles. The most evident measurement related to knocking is the cycle peak pressure [17]; cycles with higher peak pressures are more likely to result in knock. The authors model the relation between knock intensity and peak pressure and control the latter at a reference value that is a compromise between engine torque output and knock tendency. Exploiting the same philosophy, in [18], the authors build a gray-box model of the knock margin that proves to effectively describe the knock rate in various engine operating conditions, outperforming more traditional physics-based approaches. While both approaches are effective, they require a considerable modeling effort and do not consider engine aging, which also can change the relation between measurement data and knock intensity.

The majority of the scientific literature is based on the control of the statistical properties of the knock phenomenon. These methods are referred to as “stochastic” knock controllers. Instead of controlling a knock margin or acting on knock events, these methods control the statistical properties of a knock intensity metric. One possibility consists of quantifying the knock intensity

through engine casing acceleration to build a knock energy indicator controlled via a proportional integral (PI) controller acting on the spark timing [19]. The method requires the estimation of the mean and the variance of the acceleration signal energy which slows the controller action. Similar approaches based on the statistical properties of knock intensity [20] and combustion stability [21], aim at improving controller responses by adding fast control actions.

An alternative approach consists of modeling and controlling the statistical properties of knock events based on the comparison of the knock intensity metric with a calibrated threshold [16]. This approach neglects the knock intensity information and uncouples the latter from the control action intensity, but it simplifies the modeling of the knock phenomenon as knock events can be modeled by simple statistical (e.g., binomial) distributions whose characteristics are functions of the spark timing. Based on this philosophy a controller that monitors the cumulative summation of knock events and compares it with the desired knock rate is proposed in [22]. Instead of acting at each knock event by retarding the spark timing and advancing it otherwise, the controller retards the spark timing when the difference between the observed and the desired knock rate exceeds a positive threshold and advances the spark timing when the difference falls below a negative threshold. The controller presents a transient response to excess knocking events as fast as the conventional controller, but the rate of recovery from overly retarded conditions is slower. To overcome this drawback, the method is refined by using a variable threshold for enabling the controller action [23]. For both solutions, the spark timing presents a lower variance when compared to the conventional deterministic controller.

Instead of retarding and advancing the spark timing by a fixed amount ([22] and [23]), the action intensity can be related to the discrepancy between the observed and the desired knock rate. For a binomial distribution, the likelihood ratio is an indicator of the discrepancy between the observed distribution and the desired one and can be employed to modulate the retarding and the advancing actions of the controller [24]. When compared to the conventional controller, the so-called likelihood-based approach shows good results on both simulation end experimental data [25]. Although effective, stochastic knock controllers require non-trivial tuning procedures and have a delayed transitory response.

In this work, three strategies are proposed that improve deterministic and stochastic controllers. The first method improves the performance of the conventional strategy by introducing a logarithmic advance of the spark timing during non-knocking cycles. It achieves more advanced average and lower variances of the spark timing while preserving the simplicity of the conventional

strategy. The second and third methods are adaptive strategies that combine the advantages of deterministic controllers (i.e., fast action, easy implementation, and tuning) with the enhanced performance of stochastic controllers. The methods are tested and compared on an engine-validated knock stochastic simulator and an experimental test bench, outperforming both the conventional and a benchmark stochastic strategy.

The paper is organized as follows: Section II presents an overview on the knock phenomenon and its stochastic modeling. Section III proposes a new deterministic controller. Section IV introduces the full adaptive scheme combining deterministic controllers with a stochastic adaption of the parameters. In Section V, the simulation results and a comparison are discussed. In Section VI the experimental results are analyzed. The paper ends with some concluding remarks.

II. Stochastic Knock Modeling

Knock events are characterized by high pressure and temperature peaks. The most evident effect of knock occurrence is the pressure oscillation in the combustion chamber, whose amplitude is strongly related to the knock intensity. The pressure oscillation can be isolated by properly band-filtering the pressure signal and is used to establish various knock metrics. Here, the MAPO (maximum amplitude of pressure oscillation) is considered [26]. This metric is the one most commonly used in the literature and in industry due to its easy implementation and its good capabilities in evaluating knock intensity. Two examples of the cylinder pressure recorded during a knocking and a non-knocking combustion cycle are shown in Figure 1. The knock pressure oscillation is clearly detectable with a band-pass filter. The frequency range excited by knock events is 5–22 kHz and is consistent with chamber resonance frequencies given by the physical parameters of the engine [27].

Knock is a stochastic phenomenon and its intensity (e.g., MAPO) has a log-normal distribution whose properties depend on the spark timing. Figure 2 shows the probability density function (PDF) and the cumulative density function (CDF) of the MAPO metric for two different fixed spark timing values, here expressed in degrees before top dead center (°bTDC). Knock events are defined comparing the MAPO with a threshold, which defines the average knock rate (P) at a certain spark timing. A large threshold reduces the knock detection sensitivity and recognizes as knock only the cycles with large pressure oscillations, while a small threshold increases the detection sensitivity, but could lead to an excessive responsiveness as every cycle can be considered as a knock cycle. For the experimental test bench used in this work, a threshold value

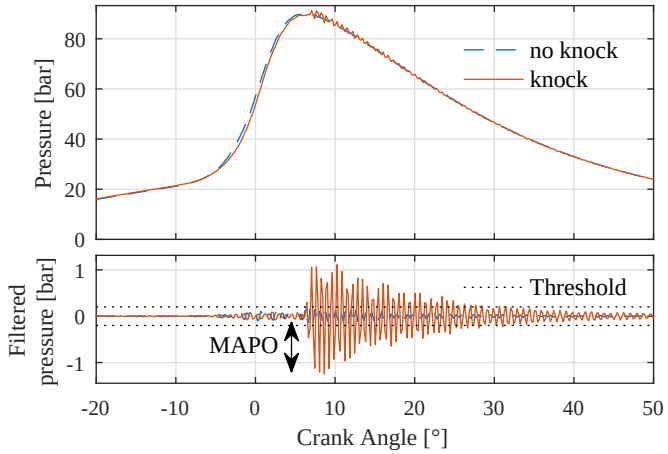

Figure 1. Pressure trace and MAPO index for knocking and non-knocking cycles with the same ignition angle.

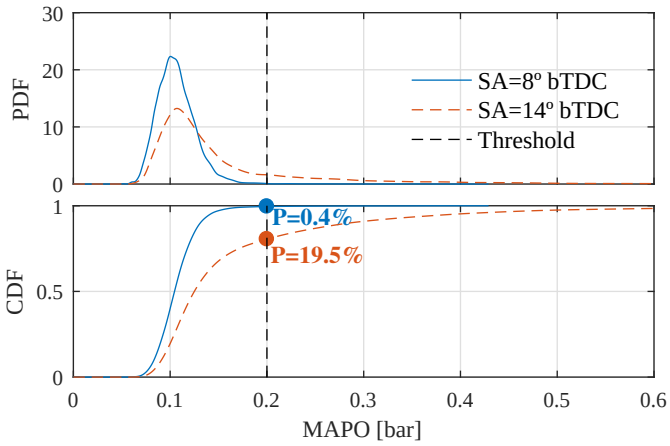

Figure 2. MAPO PDF and CDF for fixed spark angle expressed in ° bTDC. The intersection between the MAPO threshold and the CDF defines the average knocking rate at the given spark timing.

of 0.2 bar is a good compromise. Given the threshold, the static model defining the relation between the average knock rate and a constant spark timing is shown in Figure 3. Given a desired knock rate, the static model provides an indication of the average spark timing achievable. Although a proper controller design and tuning can advance the average spark timing and increase the engine efficiency for a given knock rate, it is physically limited by the characteristics of the engine.

One advantage of a discrete knock classification is the fact that knock events are binomially distributed regardless of the probability density of the knock intensity metric [28]. The latter assumption is widely acknowledged; however, it is true if the data are cyclically uncorrelated. To

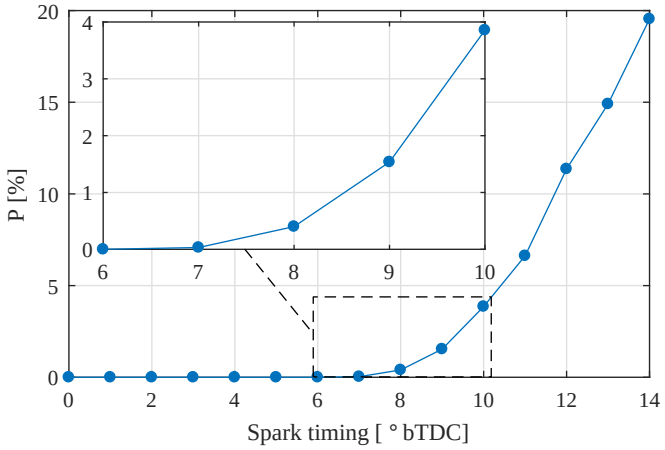

Figure 3. Average knock rate vs. fixed spark timing.

prove that the assumption holds for the MAPO index, the autocorrelation is shown in Figure 4. The analysis is performed on 200 cycles of data collected with a fixed spark timing of 14 °bTDC. Except for sporadic outliers, the rest of the data is included in the 95% probability interval. Thus, it is reasonable to assume that the MAPO index behaves as a cyclically independent random process. Based on the binomial distribution, a knock event simulator is proposed in [28]. It is

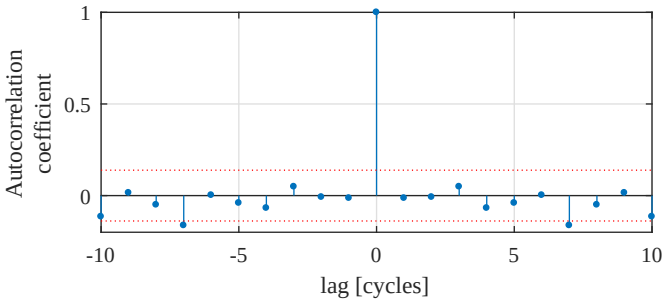

Figure 4. MAPO index autocorrelation.

used in Section V to compare the control strategies. To evaluate the reliability of the simulator, 6240 combustion cycles corresponding to a constant spark advance of 14 °bTDC are divided in 208 groups of 30 cycles each, for both experimental and simulated data. For each group, the total number of knock events is counted and the histogram is shown in Figure 5. According to the static model shown in Figure 3, a constant spark timing of 14 °bTDC corresponds to a knock rate of 19.50% and an average of 5.85 knock events per group. The results confirm that

the simulator is capable of representing the statistical properties of knock events and represents a reliable environment for comparing the controllers.

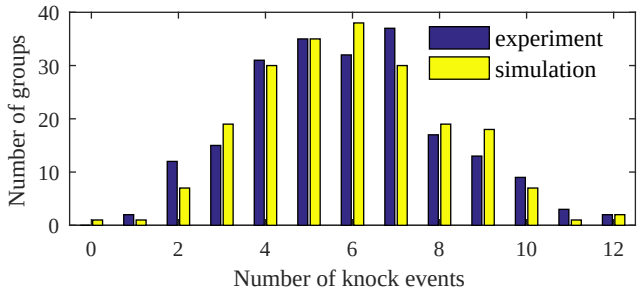

Figure 5. Histogram of knock events: simulation vs. experiment.

III. Unconventional Knock Control

The unconventional controller is based on the same principle as the conventional controller: advancing the spark timing during non-knocking cycles and retarding it on knock events. The main novelty of the unconventional strategy is the advancing rate during non-knocking cycles. It is shown that by advancing the spark timing according to a logarithmic function, the same knock rate can be achieved with a more advanced average spark timing and a lower variance. In the following, the conventional strategy is recalled, then the unconventional strategy is described and a comparison is made.

A. Conventional Strategy

Due to its easy implementation and tuning, the conventional knock controller is widely used in industrial applications. Being a deterministic controller, it acts on every knock event by retarding the spark timing while advancing it during non-knocking cycles. Equation (1)

$$S_c(j) = \begin{cases} S_c(j-1) - K_{ret} & \text{if knock,} \\ S_c(j-1) + K_{adv} & \text{otherwise,} \end{cases} \tag{1}$$

implements the strategy where $S_c(j)$ is the spark timing at cycle count j, K_{ret} is the retarding quantity on knock events, and K_{adv} is the advancing quantity during non-knocking cycles. Under the assumption of stable operation (i.e., knock occurs deterministically at a fixed spark timing), advances and retards of the controller cancel each other, and the controller parameters (i.e., K_{ret}

and K_{adv}) are related to the desired knock probability (P_{ref}) by to the following equation (see [28]):

$$K_{adv} = \frac{P_{ref}}{1 - P_{ref}} K_{ret}. \tag{2}$$

While P_{ref} is a design parameter related to the structural strength of the engine, the variable K_{ret} can be considered as a control parameter and determines the reactivity of the controller. Large values of K_{ret} allow for shorter controller transients, but increase the variance and retard the average of the spark timing at steady-state operation. From an alternative point of view, the conventional strategy searches for the average spark timing that induces the desired value of P_{ref}, resulting in a sawtooth wave. The amplitude of K_{ret} determines the searching speed and the resulting accuracy (i.e., oscillation amplitude near the average spark timing). Figure 6 shows three examples of the spark timing evolution starting from a retarded condition and under the assumption of stable operation. The examples use a desired probability of $P_{ref} = 1\%$, which corresponds to $N_{ref} = \left\lfloor \frac{1}{P_{ref}} \right\rfloor = 100$ cycles between consecutive knock events. The time required by the algorithm to reach the knocking spark (5°) decreases with large values of K_{ret}, while the oscillation of the spark at steady state increases. Therefore, K_{ret} is used to find a proper compromise between the reacting speed of the algorithm and the spark timing variation, which is reflected in cycle-to-cycle combustion variations.

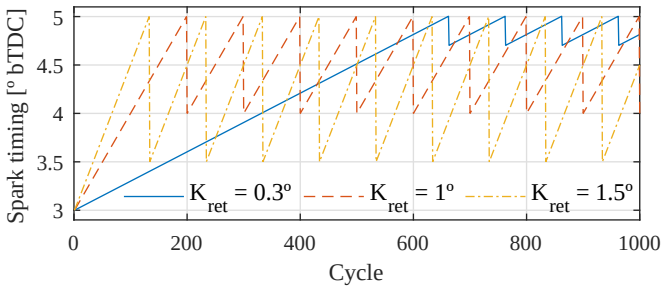

Figure 6. Examples of the evolution of the conventional controller under the assumption of stable operation. $P_{ref} = 1\%$, $N_{ref} = 100$ cycles.

B. Unconventional Strategy

The conventional strategy advances the spark timing during non-knocking cycles at a constant rate (K_{adv}). The unconventional strategy is based on the same principle, however, during non-knocking cycles the spark timing is advanced according to a logarithmic function (i.e., with a

varying rate). Its operation is based on the idea that the occurrence of consecutive knock events is rather improbable. Following a negative K_{ret} step due to a knock event, the spark timing can be advanced faster. When the number of cycles from the last knock occurrence approaches N_{ref} the advancing rate is decreased. This is implemented by the following equation:

$$S_u(j) = \begin{cases} S_u(j-1) - K_{ret} & \text{if knock,} \\ S_u(j_k) + K_{ln} \ln(c) & \text{otherwise,} \end{cases} \tag{3}$$

where K_{ln} is a tuning parameter, j_k is the cycle count of the last knock event, $S_u(j_k)$ is the spark advance applied at the last knock cycle, and c is the number of cycles since the last knock event. The variable K_{ret} here has the same function as for the conventional controller and, under the assumption of a stable operation, is related to K_{ln} and the desired knock rate. Given P_{ref} and K_{ret}, the value of K_{ln} is determined by the following equation:

$$K_{ln} = \frac{K_{ret}}{ln\left(\frac{1-P_{ref}}{P_{ref}}\right)}. \tag{4}$$

Equation (4) ensures that the knocking spark timing is reached N_{ref} cycles after the last knock event, corresponding to the desired probability. Figure 7 shows a typical spark timing evolution of the two controllers, assuming that knock events occur at $S_k = 5$ °bTDC. Both controllers

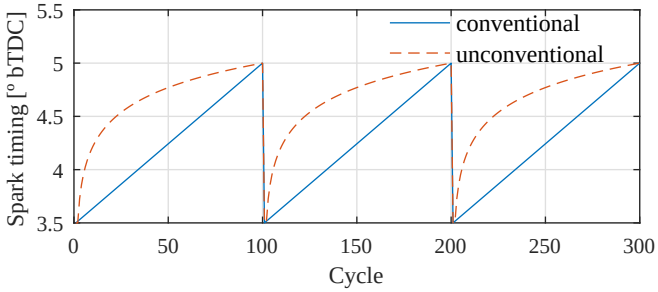

Figure 7. Unconventional vs. conventional controller evolution. $K_{ret} = 1.5°$, $P_{ref} = 1\%$ and $N_{ref} = 100$ cycles.

reach the knocking timing in N_{ref} cycles, but the difference is in the shape used to advance the spark timing, which determines the average and the variance of the control action.

C. Deterministic analysis

Under the assumption of stable operation, (i.e., evolutions as shown in Figure 7) the advantages of the unconventional controller can be computed analytically. The average and the variance of

the conventional controller spark timing are given by the following equations:

$$E\left[S_c\right] = S_k - K_{ret} + \frac{1}{N_{ref}} \sum_{j=0}^{N_{ref}-1} S_c\left(j\right) = S_k - \frac{K_{ret}}{2}, \tag{5}$$

$$VAR\left[S_c\right] = \frac{1}{N_{ref}} \sum_{0}^{N_{ref}-1} \left(S_c\left(j\right) - E\left[S_c\right]\right)^2 = \frac{K_{ret}^2}{12}. \tag{6}$$

These equations confirm that increasing K_{ret} retards the average spark timing (i.e., reduces the engine efficiency) and increases its variance. Analogously, the computation of the average and variance for the unconventional controller is given by Equations (7) and (8), which show a twofold dependence of the spark timing characteristics on K_{ret} and $P_{ref} = 1/N_{ref}$,

$$E\left[S_u\right] = S_k - K_{ret} + \frac{1}{N_{ref}} \sum_{0}^{N_{ref}-1} S_u\left(j\right) = S_k - \frac{K_{ret}}{\ln(N_{ref})}, \tag{7}$$

$$VAR\left[S_u\right] = \frac{1}{N_{ref}} \sum_{0}^{N_{ref}-1} \left(S_u\left(j\right) - E\left[S_u\right]\right)^2 = \frac{K_{ret}^2}{\ln(N_{ref})^2}. \tag{8}$$

A more evident view of the interdependence of tuning parameters and spark timing characteristics is shown in Figure 8. The advantages of the unconventional controller tend to increase for high values of K_{ret}. However, for large values of P_{ref} the unconventional control variance is higher than the conventional one. To find the upper bound of the P_{ref} range where the use of the unconventional controller is advantageous, Equations (6) and (8) can be combined, yielding a value of $\approx 3\%$. Given the definition of knock events presented in Section II and the MAPO

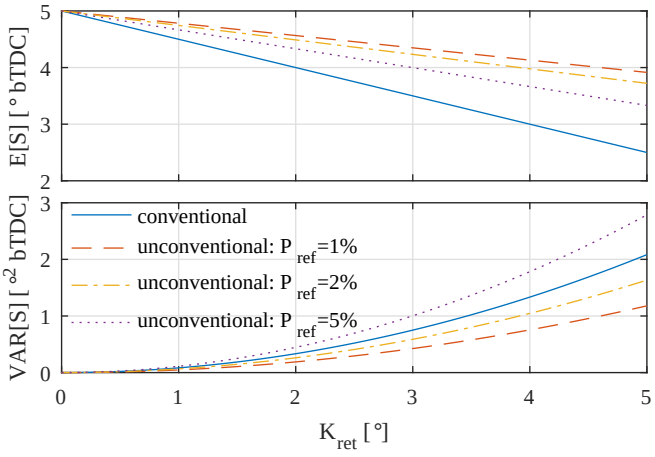

Figure 8. Analytic spark timing average ($E\left[S\right]$) and variance ($VAR\left[S\right]$) of the conventional and unconventional controllers for different values of K_{ret} and P_{ref}.

threshold chosen, a typical range found in the scientific literature for P_{ref} is 0.1% to 2%, in which the use of the unconventional controller is advantageous.

An important aspect characterizing both controllers is the settling time following a wrong initialization or a deviation from steady-state operation. Under the assumption of a stable operation, the settling time required by the conventional as well as by the unconventional algorithm to reach the knocking spark from a retarded condition is given by Equations (9) and (10), respectively:

$$T_c^{ret} = \frac{S_d \cdot (1 - P_{ref})}{K_{ret} \cdot P_{ref}}, \tag{9}$$

$$T_u^{ret} = e^{\frac{S_d \cdot \ln \frac{1-P_{ref}}{P_{ref}}}{K_{ret}}}, \tag{10}$$

where $S_d = S_k - S(0)$ is the difference between the knocking spark and the starting spark (i.e., positive values indicate a retarded initialization). Figure 9 shows a graphical representation of the two equations. It indicates that a wrong initialization combined with a low speed requirement can inhibit the controller's action and indefinitely increase the time required to reach steady-state operation, resulting in retarding the average of the spark timing and a reduced engine efficiency. This characteristic is more evident for the unconventional controller. Examples of the

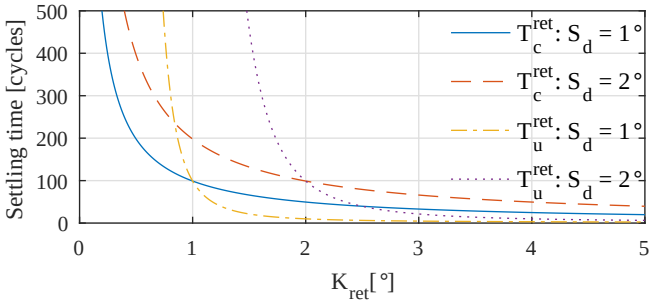

Figure 9. Settling time of the conventional controller (T_c) and the unconventional controller (T_u) under the assumption of stable operation for different values of K_{ret} and starting offset (S_d).

time-domain behavior of the unconventional strategy starting from a retarded condition and with various requirements of speed (K_{ret}) are shown in Figure 10.

Considering the initialization from an advanced condition, the time needed by the strategies to reach steady state is equal (i.e., both control strategies use the same retarding amplitude) and is given by the following:

$$T_c^{adv} = T_u^{adv} = -\left\lceil \frac{S_d}{K_{ret}} \right\rceil, \tag{11}$$

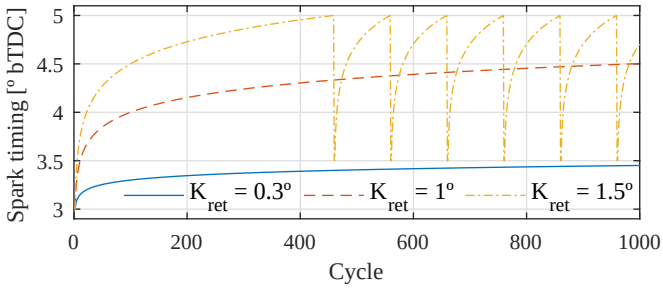

Figure 10. Examples of the unconventional controller evolution under the assumption of stable operation. $P_{ref} = 1\%$, $N_{ref} = 100$ cycles.

where S_d is the initial discrepancy w.r.t. the steady state and is negative when starting with an advanced initialization. Equation (11) evidences a positive aspect; namely the recovery time from an advanced conditions is much shorter than the recovery time from a retarded condition. Therefore, both strategies tend to be more reactive to dangerous than to low-efficiency conditions.

IV. Adaptive Knock Control

The conventional and unconventional controllers both are easy to implement and tune, but they do not employ any statistical information on knock events and they act deterministically to every knock occurrence. For both controllers, P_{ref} determines the average knock rate and K_{ret} determines the speed of the controller. Large values of K_{ret} allow for fast transients at the cost of a high variability of the control variable.

The idea of the adaptive strategy is to employ stochastic information in order to attenuate the reaction of the controller at steady state (i.e., when the stochastic properties of knock occurrences are met) and to accelerate the controller response during transients. In contrast to other studies that develop "fully" stochastic controllers, here the stochastic information of knock events is used to adapt the parameters of deterministic controllers. This combination integrates the simplicity and fast action of deterministic controllers with the enhanced information of stochastic approach.

The adaptive scheme is shown in Figure 11 and applies to both the conventional and the unconventional controller. The K_{ret} adaption block acts at a higher control level and at lower speed than the deterministic controllers. Indeed, K_{ret} is adapted at each knock event.

The adaption strategy drives K_{ret} toward a maximum value (K_{ret}^{max}) when the stochastic properties of knock occurrences are different from those desired, which enhances the convergence speed of the deterministic controllers during transients. If the stochastic properties are met, K_{ret}

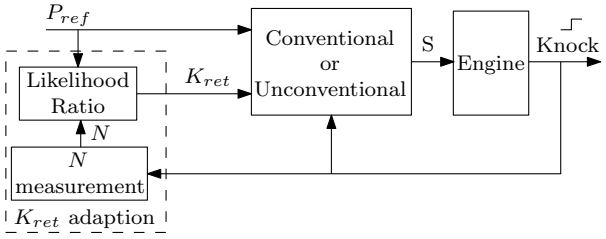

Figure 11. Adaptive knock control scheme

is driven to a minimum value (K_{ret}^{min}) in order to reduce the variance and advance the mean of the spark timing, while conserving the reaction speed of the deterministic controllers. The equation for computing K_{ret} is the following:

$$K_{ret} = K_{ret}^{min} + \left(K_{ret}^{max} - K_{ret}^{min}\right)\left(1 - L\left(N\right)\right), \tag{12}$$

where $L\left(N\right)$ is the likelihood ratio used as an indicator of the discrepancy between the expected and the measured stochastic properties of knock. The equation computing $L\left(N\right)$ is the following:

$$L\left(N\right) = \frac{\left(P_{ref}\right)^{N_k}\left(1 - P_{ref}\right)^{N - N_k}}{\left(P_{meas}\right)^{N_k}\left(1 - P_{meas}\right)^{N - N_k}}, \tag{13}$$

where N_k is the number of past knock events considered, N is the number of cycles in which N_k events occurred, $P_{meas} = N_k/N$ is the sampled probability, and P_{ref} is the reference probability. The ratio $L\left(N\right)$ can be interpreted as the probability of obtaining N_k events in N samples of a binomial stochastic process with the nominal probability P_{ref}. For instance, given a desired probability of 1% (see example shown in Figure 12), the likelihood ratio is greatest when the distance between the last two knock events ($N_k = 1$) is equal to 100 cycles, or the last three events ($N_k = 2$) occur in 200 cycles. Among the quantities involved in Equation (13), P_{ref} and N_k are tuning parameters and N is measured. For further details, the reader is referred to [24], [29]. Compared to deterministic controllers, the adaption of K_{ret} operates at a lower speed and the number of past knock events considered in the likelihood ratio computation (N_k) determines the memory of the adaption strategy. Values of N_k larger than 1 would reduce the variability of the spark timing at the cost of a longer settling time. In the simulations and experiments that follow, a fixed value of $N_k = 1$ is used.

The adaptive strategies have three tuning parameters. Because P_{ref} and K_{ret}^{max} are equivalent to P_{ref} and K_{ret} of the non-adaptive strategies, the tuning of these two parameters requires just a minimal effort as they are not related and determine different aspects of the controllers. The

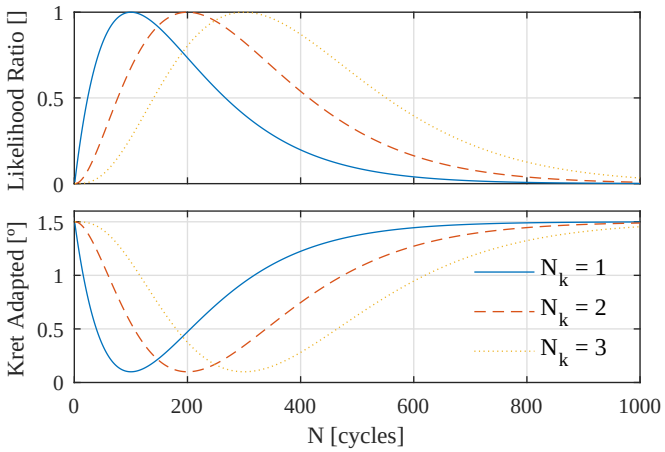

Figure 12. Likelihood ratio and K_{ret} adapted. $P_{ref} = 1\%$, $K_{ret}^{min} = 0.1$ and $K_{ret}^{max} = 1.5$

variable K_{ret}^{min} determines the operation of the adaption rule; if $K_{ret}^{min} = K_{ret}^{max}$, the action of the adaptive rule is inhibited, and if $K_{ret}^{min} = 0$ the controller action is frozen when the stochastic properties of knock are met. The value of K_{ret}^{min} should be chosen based on the minimum reaction speed desired for the controller.

V. Simulation results

In this section the proposed controllers are compared with the conventional strategy and a stochastic benchmark controller presented in Section V-A. Unlike Section III, where the controllers are analyzed on deterministic conditions, in this section the comparison is made using the stochastic knock simulator presented in Section II. The comparison includes steady-state operation (Section V-B) and transitory behavior (Section V-C) starting from retarded and advanced conditions. The tuning of the adaption rule is analyzed in Section V-D.

A. *Benchmark stochastic control*

In addition to the conventional strategy, the methods proposed in this paper are compared with a "fully" stochastic controller based on the likelihood ratio, as presented in [24]. The basic version of the benchmark controller acts on the spark timing if $L(N) < L_{th}$, that is, if the measured stochastic properties do not match the desired ones. If the measured probability (P_{meas}) exceeds the reference probability (P_{ref}), the spark timing is retarded by $K_{ret} \cdot (1 - L(N))$, otherwise it is advanced by $K_{adv} \cdot (1 - L(N))$. Hence, compared to deterministic controllers, the benchmark

controller preserves its output until a new knock event occurs, presenting a lower variability but a slower response. The likelihood ratio threshold (L_{th}), as well as K_{adv}, K_{ret} and P_{ref} are tuning parameters. Unlike the conventional strategy, the variables K_{adv} and K_{ret} are not related to the reference probability, which makes the tuning process more difficult. Additionally, the algorithm presents a slow response after long periods of operation at the desired target. To cope with this drawback, a modified version of the algorithm is proposed. In this work, the modified version, Algorithm 1 (corresponding to Algorithm 3 in [24]), is used as a benchmark.

B. Steady-state operation

In this section, the proposed controllers, the conventional and the benchmark controller are compared in steady-state operation. The reference point considered in the comparison is at a knock rate of 1% with the nominal value of K_{ret} of the conventional and the unconventional controller being equal to 1.5 °. The value of K_{ret}^{max} for the adaptive strategies is also set to 1.5 ° in order for the maximum speed to be equal to that of the non-adaptive strategies. The values of the parameters K_{ret} and K_{adv} of the benchmark controller are tuned to obtain an average knock rate of approximately 1%, while the likelihood ratio threshold (L_{th}) is set to the same value as that of the reference paper. The values of the parameters for all the controllers are summarized in Table I.

Table I

CONTROLLER PARAMETERS FOR THE REFERENCE POINT COMPARISON

	conv	**unconv**	**ad conv**	**ad unconv**	**bench**
P_{ref}	1%	1.5%	1%	1.5%	1%
K_{ret}	1.5°	1.5°	online	online	0.5°
K_{ret}^{max}	-	-	1.5°	1.5°	-
K_{ret}^{min}	-	-	0.1°	0.1°	-
K_{adv}	0.015	-	online	-	1.25°
K_{ln}	-	0.3264	-	online	-
L_{th}	-	-	-	-	0.4

The controllers were simulated for $25 \cdot 10^3$ cycles and the average results are shown in Table II. Under steady-state conditions the proposed controllers outperform both the conventional and the benchmark controller. While the improvement in terms of average spark timing (i.e., engine efficiency) is limited by the engine characteristics, the improvement in terms of spark timing

Algorithm 1 Benchmark likelihood-based control

Initialize knockEventCount = 0;
Initialize FIFO buffer to store cycleCounts = $\{0, 0, 0, 0\}$;
Initialize criticalCycleCounts, $n_k = \{92, 18, 65, 123\}$;
...
if knocking **then**
  Increment knockEventCount up to a maximum count of 3;
  Right-shift the FIFO buffer by one place, (left-fill with 0);
end if

for i=0 to knockEventCount **do**
  Increment cycleCounts(i);
  if (i=0)&(cycleCounts(i)≥criticalCycleCounts(i)) **then**
    P_{meas} = knockEventCount/cycleCounts(i);
    Compute likelihood ratio ($L\,(N)$) for i events in cycleCounts(i) cycles;
    Increment spark by $K_{adv} \cdot (1 - L\,(N))$;
    Reset the knockEventCount to zero;
    Reset all elements of cycleCounts to zero;
  else
    if (i=0)&(cycleCounts(i)≤criticalCycleCounts(i)) **then**
      P_{meas} = knockEventCount/cycleCounts(i);
      Compute likelihood ratio ($L\,(N)$) for i events in cycleCounts(i) cycles;
      Decrement spark by $K_{ret} \cdot (1 - L\,(N))$;
      Reset the knockEventCount to zero;
      Reset all elements of cycleCounts to zero;
    end if
  end if
end for

variability is considerable. Considering this aspect, the adaptive unconventional controller shows the best performance.

Table II

SIMULATION RESULTS AT STEADY-STATE OPERATION

	conv	**unconv**	**ad conv**	**ad unconv**	**bench**
$E[P]\,(\%)$	1.00	0.99	1.04	1.01	1.04
$E[S]\,(^\circ)$	8.35	8.48	8.64	8.56	8.30
$VAR[S]\,(^{\circ 2})$	0.71	0.30	0.30	0.13	0.37

The first 1000 cycles of a simulation are shown in Figure 13. The four advanced controllers (i.e., benchmark, unconventional, adaptive conventional and adaptive unconventional) are compared with the conventional controller (dashed line). The two deterministic controllers have the most straightforward behavior; both retard the timing on knock events and advance it otherwise. The conventional controller advances the timing linearly, while the unconventional controller advances it logarithmically. The benchmark controller is a fully stochastic controller, hence it does not act at each cycle and changes the spark timing only when the likelihood ratio overshoots the threshold. The adaptive strategies retard the timing depending on the discrepancy between the expected and the measured cycles between two consecutive knock events. This behavior is highlighted by the varying amplitude of the retarding action on knock events.

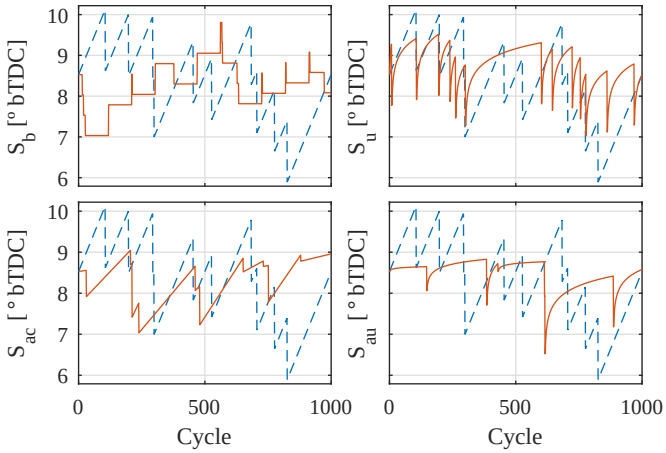

Figure 13. Simulation example at steady-state operation. In each subplot, the conventional controller (dashed line) is compared with the benchmark (top left), the unconventional (top right), the adaptive conventional (bottom left) and the adaptive unconventional controller (bottom right).

A clearer evidence of the differences between the actions of the controllers action is provided by the histogram of the spark timing. Figure 14 shows the histogram of the presented and the benchmark controllers (solid black) and compares them with the conventional controller (light yellow). All the proposed controllers have a narrower distribution than the conventional and benchmark controllers. The best performing controller is the adaptive unconventional one, as confirmed by its low variance.

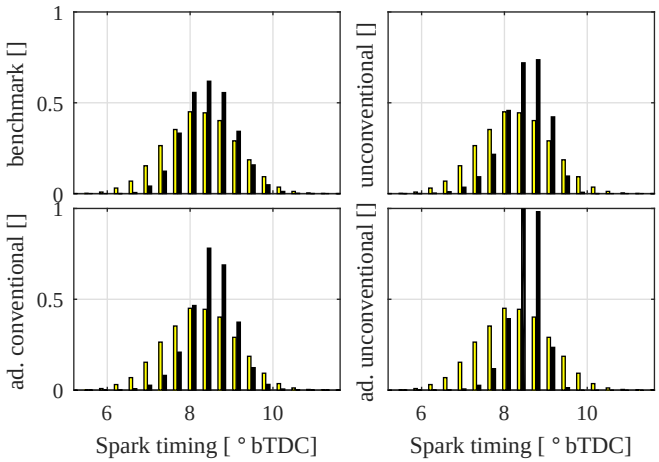

Figure 14. Comparison of the spark timing distribution.

Another important aspect of the controllers is the discrepancy between the required knock rate and the resulting average rate. In this sense, the conventional controller shows the best behavior (Figure 15) as it achieves negligible errors on the resulting average rate. The adaptive conventional controller preserves this property. The unconventional controllers and the benchmark require appropriate tuning and/or scheduling to match the desired rate. However, while the unconventional strategies require only the tuning of P_{ref}, the parameters of the benchmark controller are coupled, which complicates its tuning.

The advantages of the proposed controllers are evidenced by executing the comparison under steady-state conditions for different values of the reference probability (P_{ref}) and controller speed (K_{ret} and K_{ret}^{max}). As expected, the average spark timing (Figure 16) of all controllers is close to the static map (i.e., the identified engine model presented in Figure 3). The improvement of the average spark timing thus is limited by the system properties. However, requiring a high controller speed (K_{ret} and K_{ret}^{max} equal to 3°) affects the resulting average timing of the non-adaptive strategies, whereas the effect on the adaptive strategies is negligible. The most evident

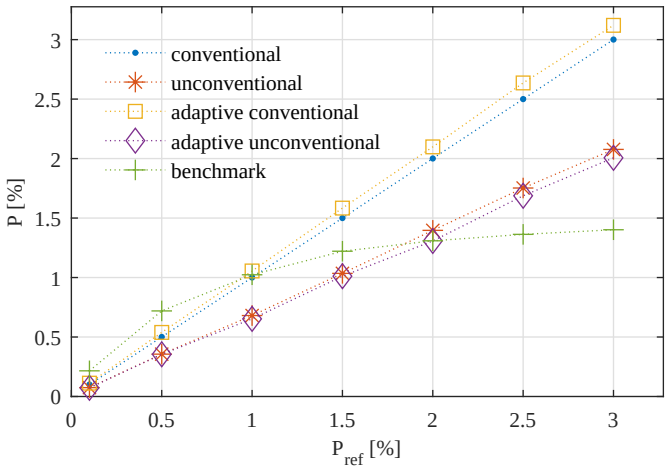

Figure 15. Actual knock rate (P) vs. reference probability (P_{ref}). The other parameters are equal to the values used for the reference point.

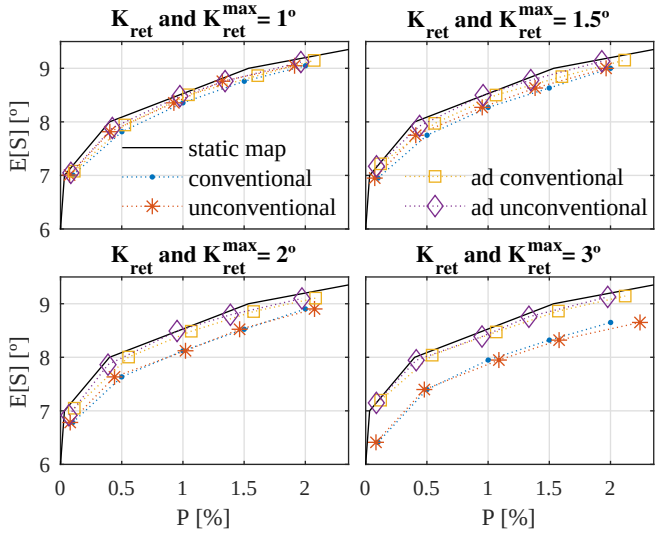

Figure 16. Spark timing average for different values of K_{ret}, K_{ret}^{max} and P_{ref}. For the adaptive strategies $K_{ret}^{min} = 0.1$.

effect of high-speed tuning is the increase of the variability of the control action (Figure 17). As expected from the deterministic study (Equation (6)), the variance of the conventional control output is strongly affected by K_{ret}, while the increase of the unconventional output is less affected. The adaptive strategies present a limited influence on the controller speed and allow for a more advantageous trade-off between speed and output variability.

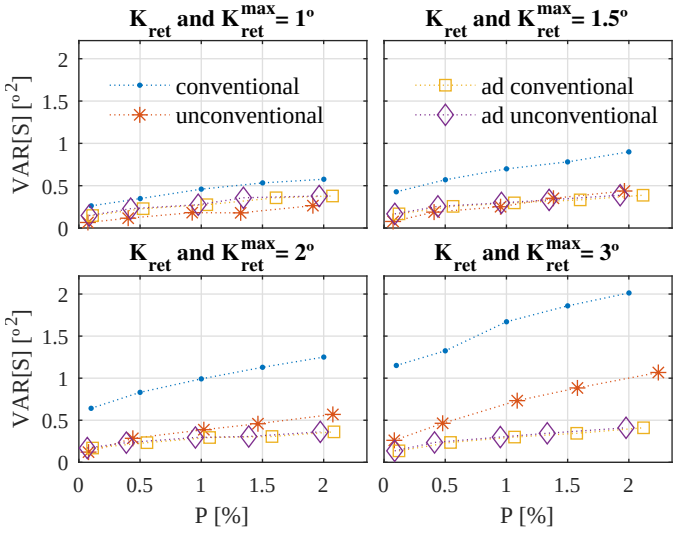

Figure 17. Spark timing variance for different values of K_{ret}, K_{ret}^{max} and P_{ref}. For the adaptive strategies $K_{ret}^{min} = 0.1$.

C. Transitory operation

The settling time is an important aspect in controller design. A short settling time means a quick adaption to changes in the engine characteristics or in the desired probability. In the methods proposed, this goal is achieved by combining a stochastic adaption of the parameters with deterministic controllers, which yield a fast response.

Here, the settling time is analyzed by looking at the time required to reach steady-state conditions starting from a retarded or an advanced condition. Since all controllers advance and retard the spark timing differently, both initial conditions are considered. The controller parameters are the same as those used in the steady-state analysis, and the average knock rate is 1%. According to the static engine relation (Figure 3), the expected average spark timing at the 1% rate is 8.53 ºbTDC. For each controller, the settling time is computed as the time needed to intersect the expected average.

Figure 18 shows a simulation example of the controller responses starting from an advanced condition (i.e., 2° w.r.t. the expected average). The three controllers introduced and the benchmark controller (solid lines) are compared with the conventional control (dashed line). As can be expected, the conventional controller is the fastest, followed by the adaptive conventional controller. The adaptive unconventional controller presents a slower response, while the unconventional controller behaves better than the stochastic controller. The results confirm the conclusions of the deterministic study, namely the fact that the logarithmic shaping of the spark timing reduces

the variance of the control action in exchange for slower speed.

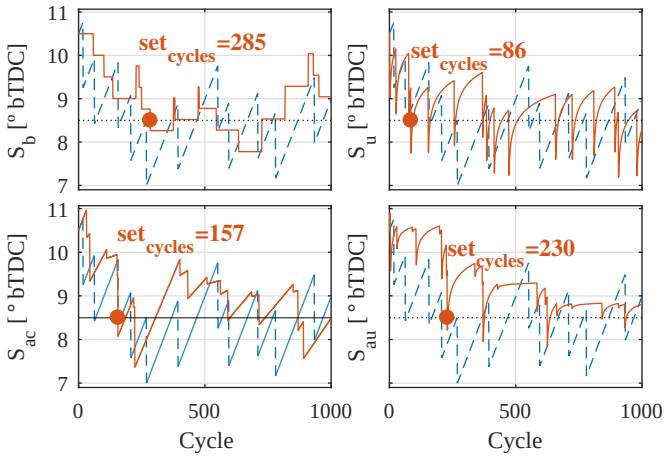

Figure 18. Settling time starting from advanced timing. The conventional controller shows a settling time of 64 cycles.

Figure 19 shows a simulation example of the controller responses starting from a retarded condition (i.e., 2° w.r.t. the expected average). The results are similar to those of the advanced condition and the controllers show the same order of the performances. The conventional and the adaptive conventional are the fastest controllers, while the adaptive unconventional one is the slowest. The benchmark and the unconventional controllers present intermediate results.

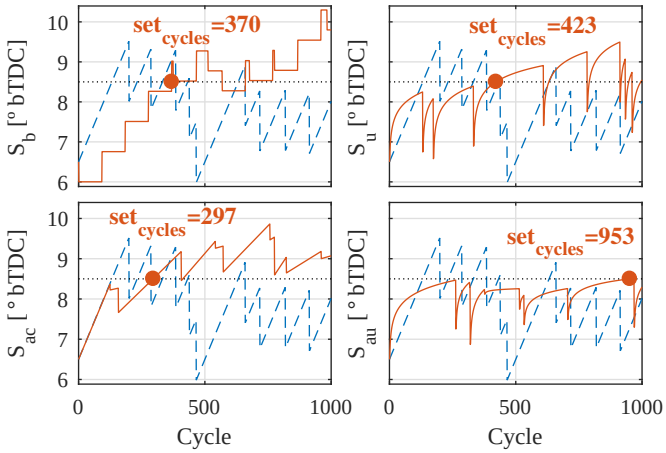

Figure 19. Settling time starting from retarded timing. The conventional controller presents a settling time of 133 cycles.

Given the stochastic nature of knock (and the knock simulator), the results of the settling time vary for each simulation. To better evaluate the differences between the controllers, 1000 simulations have been run for both starting conditions. The average results are summarized in

Table III. They confirm that among the proposed controllers the adaptive conventional one is the fastest. While its times are longer than those of the conventional controller, it outperforms the stochastic controller. The unconventional controller presents a twofold behavior: its settling time when starting from advanced conditions is low, almost as low as that of the conventional controller, and it is slow when starting from a retarded condition. The adaptive unconventional is the slowest controller in both conditions. Therefore, the unconventional controllers, both the non-adaptive and the adaptive versions, are most suitable for steady-state conditions, while the adaptive conventional controller is suitable for both transitory and steady-state behavior and provides the best trade-off between variability and speed.

Table III
RESULTS OF SETTLING TIME ANALYSIS (1000 SIMULATIONS)

Strategy	**Advanced start**	**Retarded start**
Conventional	64 cycles	177 cycles
Unconventional	86 cycles	423 cycles
Adaptive conventional	157 cycles	299 cycles
Adaptive unconventional	230 cycles	953 cycles
Benchmark	285 cycles	351 cycles

As expected from the deterministic analysis, the controllers present different settling times when starting from an advanced or a retarded condition. On the one hand, this behavior is due to the different amplitudes of the advancing and retarding actions (i.e., K_{adv} and K_{ret}), while on the other hand, this behavior is a consequence of the nonlinearities of the relation between knock rate and spark timing (Figure 3).

D. Stochastic adaption tuning

The conventional controller and those proposed in this work share the same tuning parameters, where P_{ref} determines the knock rate, K_{ret} determines the reactivity of the conventional and unconventional controllers, and K_{ret}^{max} and K_{ret}^{min} determine the maximum and the minimum reactivity of the adaptive controllers. In this section, the proposed controllers are compared with the conventional one at a fixed value of P_{ref} and for different values of K_{ret}, K_{ret}^{max} and K_{ret}^{min}. The target is to explore more favorable trade-offs between the controller speed and the spark timing variability. The values of K_{ret} and K_{ret}^{max} thus are intentionally chosen to be equal in order

to have the maximum speed of the adaptive strategies equal to the speed of the non-adaptive ones.

Figure 20 shows the sensitivity results of the non-adaptive strategies to K_{ret} and of the adaptive strategies to K_{ret}^{max}. These results are obtained by averaging 1000 simulations to avoid any stochastic variations of the settling time and to show that by changing K_{ret} and K_{ret}^{max}, it is possible to achieve settling times that are as short as those of the conventional controller while reducing the variability of the spark timing by more than 50%.

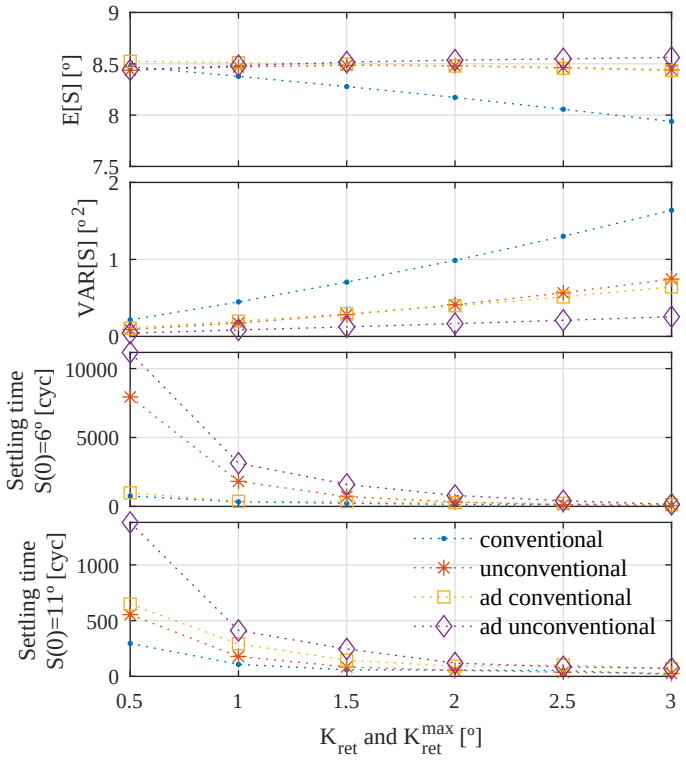

Figure 20. Sensitivity to K_{ret} and K_{ret}^{max} (the other parameters are equal to those shown in the steady-state comparison).

The action of the adaptive strategy depends on the value of K_{ret}^{min}, which determines the amplitude of the adaption (i.e., the variation range of K_{ret}). The sensitivity to K_{ret}^{min} is shown in Figure 21. Again, the results are obtained by averaging 1000 simulations. As expected, when the value of K_{ret}^{min} approaches that of K_{ret}^{max}, the effect of the adaptive rule vanishes and the adaptive controllers behave the same way as their non-adaptive counterparts. Low values of K_{ret}^{min} allow for a better performance, whereas a choice of $K_{ret}^{min} \approx 0$ can indefinitely freeze the controller action if the stochastic properties are met during transients.

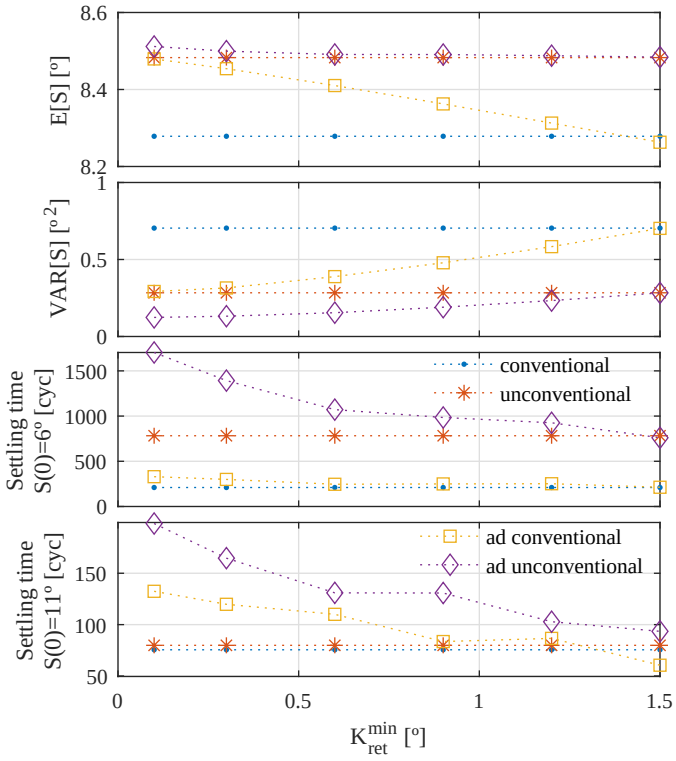

Figure 21. Sensitivity to K_{ret}^{min} (the other parameters are equal to those of the steady-state comparison).

VI. Experimental results

The performances of the controllers are compared on a test bench equipped with an electric brake and a four-stroke SI engine. The engine is equipped with a turbocharger, a variable valve camshaft, and direct gasoline injection. Injection timing was set at 270 °bTDC and intake valve closing was set at 180 °bTDC. The main characteristics of the engine are summarized in Table IV. The air-to-fuel ratio is measured by a sensor at the exhaust and is regulated at stoichiometric

Table IV
Main engine characteristics

	Units	Value
Cylinders	[-]	3
Combustion type	[-]	SI
Unitary displacement	[cc]	499.6
Bore	[mm]	82
Compression ratio	[-]	10.1:1

conditions by closed-loop-controlling the amount of fuel injected. The air mass flow is measured by a hot-film anemometer and controlled by a waste-gate valve at the turbocharger. All the tests are performed at a speed of 1500 rpm, an air mass flow equal to 667 mg/stroke, a coolant temperature of 85 °C, and a rail pressure of 200 bar.

Each controller is tested in steady-state and transitory conditions, using the same tuning parameters as those used for the simulations.

A. Steady-state operation

The average results of the steady-state experiments ($25 \cdot 10^3$ cycles) are summarized in Table V. The results confirm those obtained in the simulations. The adaptive strategies present the best behavior with the most advanced timing and the lowest variance. As with the simulator, the conventional and the adaptive conventional controllers show the best match between the required and the resulting knock rate.

Table V
EXPERIMENTAL RESULTS AT STEADY-STATE OPERATION

	conv	**unconv**	**ad conv**	**ad unconv**	**bench**
$E[P]\,(\%)$	1.00	1.08	1.01	1.07	1.04
$E[S]\,(^\circ)$	8.22	8.27	8.51	8.47	8.13
$VAR[S]\,(^{\circ 2})$	0.71	0.29	0.40	0.11	0.44

The first 1000 cycles of the experiments are shown in Figure 22, while the histogram of the spark timing distribution is shown in Figure 23. The graphs in both figures are similar to the results obtained with the stochastic simulator and represent a further validation of the accuracy of the simulator. The behavior of the adaptive strategies indicates that reducing the reaction of the event-based controllers is effective.

B. Transitory behavior

The transitory behavior is analyzed analogously to that of the simulations. The controllers are initialized with a retarded and an advanced condition; for both conditions the distance from the expected steady-state average is 2 °. The experiments have been repeated 10 times in order to reduce the effects of the stochastic behavior of knock. The results match those obtained with the simulator and the deterministic analysis of Section III. The conventional is the fastest controller.

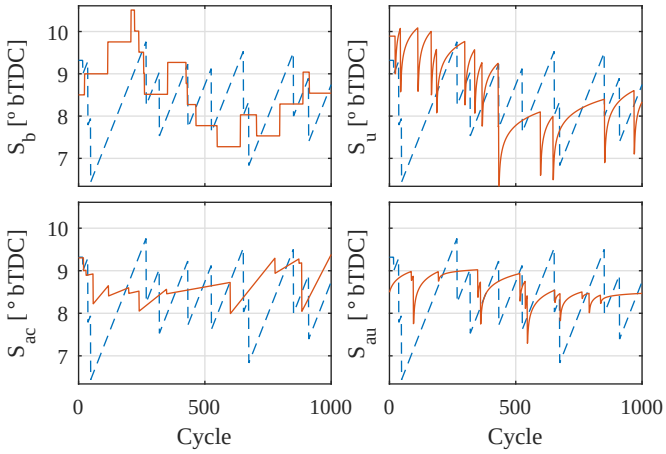

Figure 22. Experimental example at steady-state operation. In each subplot the conventional controller (dashed line) is compared with the benchmark (top left), the unconventional (top right), the adaptive conventional (bottom left), and the adaptive unconventional controllers (bottom right).

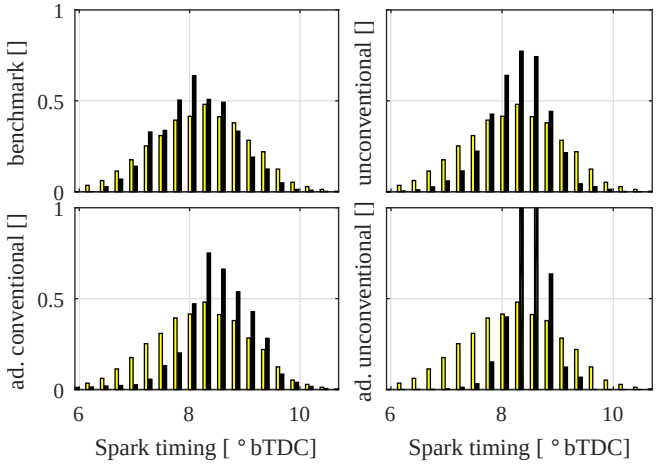

Figure 23. Comparison of the experimental PDF of the spark timing.

Among the advanced controllers, the adaptive conventional controller presents the fastest response on both starting conditions and overall shows the best trade-off between controller speed and steady-state response. The example of the time evolution of the controllers shown in Figures 24 and 25 matches the behavior on the stochastic simulator and confirms its reliability.

VII. Conclusion

Knock control is crucial for avoiding deterioration and increasing efficiency in spark-ignited engines. In this paper, three innovative controllers are proposed and compared with a conventional

Table VI

RESULTS OF SETTLING TIME ANALYSIS (10 EXPERIMENTS)

Strategy	**Advanced start**	**Retarded start**
Conventional	53 cycles	162 cycles
Unconventional	102 cycles	523 cycles
Adaptive conventional	106 cycles	287 cycles
Adaptive unconventional	181 cycles	907 cycles
Benchmark	249 cycles	328 cycles

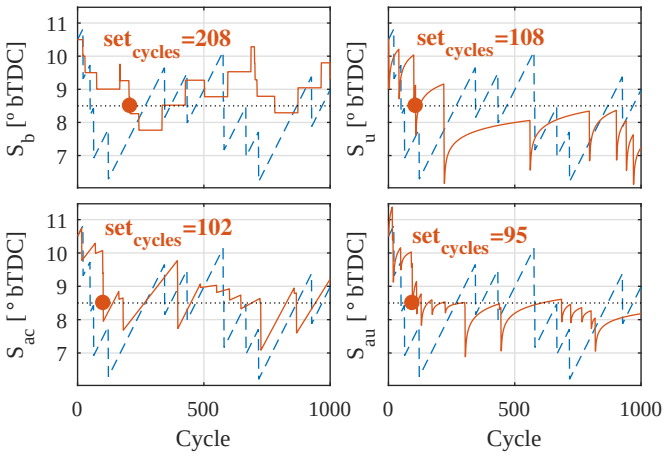

Figure 24. Evolution of the spark timing starting from advanced condition.

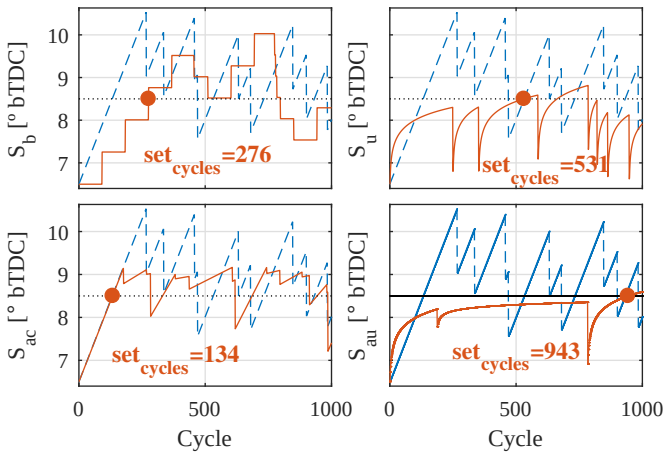

Figure 25. Evolution of the spark timing starting from retarded condition.

and a benchmark controller. The proposed strategies exploit two approaches for improving knock control.

The unconventional controller uses a modified shape of control action. Instead of advancing linearly, the controller advances the spark timing with a logarithmic shape.

The second approach consists of an adaptive strategy that applies to both conventional and unconventional controllers and aims at combining deterministic controllers with a stochastic adaption of the parameters. Using a stochastic indicator the parameters, are scheduled between a fast configuration during transients and a low-variance configuration in steady-state operation.

The three controllers are tested using a validated stochastic simulator which correctly represents the behavior of knock occurrences, and using an experimental test bench. For a fair and wide comparison, aside from the conventional strategy, a stochastic controller described in recent literature has been used as a benchmark as well.

In addition to being able to regulate the knock rate at the desired target, the results evidence that the logarithmic advancing of the spark timing allows its lowest variance to be achieved thus suitable for steady-state conditions. When the transient response is considered, the conventional controller shows the best results. Therefore, the adaptive conventional strategy should be considered as it features an optimal compromise between response time and steady-state behavior. Aside from their good performance, compared with the benchmark stochastic controller, all the controllers proposed in this work require fewer parameters to be defined and a minor tuning effort.

REFERENCES

[1] L. Guzzella and C. Onder, "Introduction to modeling and control of internal combustion engine systems," 2010.

[2] K. Kaji, S. Matsushige, M. Kanamaru, J. Takahashi, and S. Asano, "Development of knock sensor," in *SAE Technical Paper*. SAE International, October 1986.

[3] S. M. Dues, J. M. Adams, and G. A. Shinkle, "Combustion knock sensing: Sensor selection and application issues," in *SAE Technical Paper*. SAE International, February 1990.

[4] S.-H. Jang, Y.-G. Lee, T.-Y. Oh, and K.-S. Park, "An experimental study on knock sensing for a spark ignition engine," in *SAE Technical Paper*. SAE International, November 1993.

[5] E. Pipitone and L. D'Acquisto, "Development of a low-cost piezo film-based knock sensor," *Proceedings of the Institution of Mechanical Engineers, Part D: Journal of Automobile Engineering*, vol. 217, no. 8, pp. 691–699, 2003.

[6] K. Burgdorf and I. Denbratt, "Comparison of cylinder pressure based knock detection methods," in *SAE Technical Paper*. SAE International, October 1997.

[7] S. Ortmann, M. Rychetsky, M. Glesner, R. Groppo, P. Tubetti, and G. Morra, "Engine knock estimation using neural networks based on a real-world database," in *SAE Technical Paper*. SAE International, February 1998.

[8] R. Worret, S. Bernhardt, F. Schwarz, and U. Spicher, "Application of different cylinder pressure based knock detection methods in spark ignition engines," in *SAE Technical Paper*. SAE International, May 2002.

[9] J. Naber, J. R. Blough, D. Frankowski, M. Goble, and J. E. Szpytman, "Analysis of combustion knock metrics in spark-ignition engines," in *SAE Technical Paper*. SAE International, April 2006.

[10] J. M. Borg, G. Saikalis, S. Oho, and K. C. Cheok, "Knock signal analysis using the discrete wavelet transform," in *SAE Technical Paper*. SAE International, April 2006.

[11] M. Ettefagh, M. Sadeghi, V. Pirouzpanah, and H. A. Tash, "Knock detection in spark ignition engines by vibration analysis of cylinder block: A parametric modeling approach," *Mechanical Systems and Signal Processing*, vol. 22, no. 6, pp. 1495–1514, 2007.

[12] G. Wu, "A real time statistical method for engine knock detection," in *SAE Technical Paper*. SAE International, April 2007.

[13] Y. Lonari, C. Polonowski, J. Naber, and B. Chen, "Stochastic knock detection model for spark ignited engines," in *SAE Technical Paper*. SAE International, April 2011.

[14] E. Galloni, "Dynamic knock detection and quantification in a spark ignition engine by means of a pressure based method," *Energy Conversion and Management*, vol. 64, pp. 256–262, 2012.

[15] K. Akimoto, H. Komatsu, and A. Kurauchi, "Development of pattern recognition knock detection system using short-time fourier transform," *IFAC Proceedings Volumes*, vol. 46, no. 21, pp. 366–371, 2013.

[16] U. Kiencke and L. Nielsen, *Automotive control systems: for engine, driveline, and vehicle*. Springer Science & Business Media, 2005.

[17] U. Lezius, M. Schultalbers, W. Drewelow, and B. Lampe, "Improvements in knock control," in *Mediterranean Conference on Control & Automation, 2007. MED'07.* IEEE, June 2007, pp. 1–5.

[18] G. Panzani, C. Onder, and F. Ostman, "Engine knock margin estimation using in-cylinder pressure measurements," *IEEE/ASME Transactions on Mechatronics*, pp. 1–12, 2016.

[19] M. Penese, C. F. Damasceno, A. Bucci, and G. Montanari, "Sigma® on knock phenomenon control of flexfuel engines," in *SAE Technical Paper*. SAE International, November 2005, p. 3990.

[20] N. Cavina, G. Po, and L. Poggio, "Ion current based spark advance management for maximum torque production and knock control," in *ASME 8th Biennial Conference on Engineering Systems Design and Analysis*. American Society of Mechanical Engineers, 2006, pp. 537–545.

[21] G. Zhu, I. Haskara, and J. Winkelman, "Stochastic limit control and its application to spark limit control using ionization feedback," in *Proceedings of the 2005, American Control Conference, 2005.* IEEE, June 2005, pp. 5027–5034.

[22] J. C. P. Jones, K. R. Muske, J. Frey, and D. Scholl, "A stochastic knock control algorithm," in *SAE Technical Paper*. SAE International, April 2009.

[23] J. C. P. Jones, J. Frey, and K. R. Muske, "A fast-acting stochastic approach to knock control," *IFAC Proceedings Volumes*, vol. 42, no. 26, pp. 16 – 23, 2009.

[24] J. C. P. Jones, J. M. Spelina, and J. Frey, "Likelihood-based control of engine knock," *IEEE Transactions on Control Systems Technology*, vol. 21, no. 6, pp. 2169–2180, November 2013.

[25] A. Thomasson, H. Shi, T. Lindell, L. Eriksson, T. Shen, and J. C. P. Jones, "Experimental validation of a likelihood-based stochastic knock controller," *IEEE Transactions on Control Systems Technology*, vol. 24, no. 4, pp. 1407–1418, July 2016.

[26] A. J. Shahlari and J. B. Ghandhi, "A comparison of engine knock metrics," in *SAE Technical Paper*. SAE International, October 2012.

[27] C. S. Draper, "The physical effects of detonation in a closed cylindrical chamber," 1935.

[28] J. M. Spelina, J. C. P. Jones, and J. Frey, "Stochastic simulation and analysis of a classical knock controller," *International Journal of Engine Research*, vol. 16, no. 3, pp. 461–473, 2015.

[29] H. Kobayashi, B. L. Mark, and W. Turin, *Probability, random processes, and statistical analysis*. Cambridge University Press, 2011.